J Therm Anal Calorim (2015) 120:1241–1248
DOI 10.1007/s10973-015-4397-3

Hydration properties of steel slag under autoclaved condition

Qiang Wang · Mengxiao Shi · Zengqi Zhang

Received: 21 September 2014 / Accepted: 4 January 2015 / Published online: 15 February 2015

Abstract This paper investigated the hydration properties of steel slag under autoclaved condition (216 °C and 2 MPa). The results show that under autoclaved condition, besides C_2S and C_3S, *f*-CaO and the minerals containing MgO can react sufficiently. The morphologies of $Ca(OH)_2$ produced by *f*-CaO are quite different from those produced by C_2S and C_3S. The $Ca(OH)_2$ produced by *f*-CaO has a larger specific surface area or volume than that produced by C_2S and C_3S. The mean Ca–Si ratio of the C–S–H gel produced by steel slag is between 1.7 and 1.9, which is a little smaller than that produced by cement. The reaction of *f*-CaO tends to cause greater expansion than that of the minerals containing MgO.

Keywords Steel slag · Autoclaved · Hydration · Free CaO · MgO

Introduction

Steel slag, a by-product from the steel-making process, is a potential mineral admixture for cement or concrete production [1]. C_3S, C_2S, C_4AF, and C_2F are common minerals in steel slag, which endow steel slag with cementitious properties [2, 3]. The main hydration products of steel slag include C–S–H gel and $Ca(OH)_2$, which are very similar to those of cement [4]. The active minerals of steel slag hydrate much more slowly than those of cement, because the cooling process of steel slag is very long but that of cement is rather short [5]. So steel slag tends to decrease the early strength of cement or concrete [6, 7]. But the negative effect of steel slag on the strength of concrete is weaker at the lower water-to-binder ratio, which might be due to the improving effect of steel slag on the hydration of cement at the lower water-to-binder ratio [8, 9].

When steel slag is used as a mineral admixture for cement or concrete, its activity is very important. The activity of the active components of steel slag can be improved by increasing its fineness [10]. In the meanwhile, the non-active components of steel slag can play a better role as fillers in the hardened paste by increasing the fineness of steel slag [4]. The activity of steel slag can also be improved by increasing its active components content through adding regulating components to the steel slag in the melting state [11]. High curing temperature can promote the hydration of the components with high activity and also excite the activity of low-active components such as large C_2S particles. So steel slag exhibits much higher activity under the condition of higher curing temperature [12, 13]. Autoclave curing technology is widely used in the building material products, such as brick, cement pile, and precast concrete [14–18]. The temperature of the autoclave curing technology is much higher than 100 °C, so the activity of the binder can be promoted significantly. In theory, steel slag can exhibit satisfied cementitious properties under autoclaved condition.

The soundness of steel slag is also very important when it is applied to cement or concrete. Free CaO and the minerals containing MgO are the main factors influencing the soundness of steel slag [19, 20]. If a considerable amount of free CaO and the minerals containing MgO react at the late hydration age of cement, the internal expansion caused by the formation of $Ca(OH)_2$ and $Mg(OH)_2$ might damage the microstructure of concrete. Therefore, in theory, the free CaO content and MgO content of steel slag should be strictly restricted when it is used in cement or cast-in situ concrete.

Q. Wang (✉) · M. Shi · Z. Zhang
Department of Civil Engineering, Tsinghua University, Beijing 100084, China
e-mail: w-qiang@tsinghua.edu.cn

Table 1 Properties of the steel slags used

Samples	A	B	C	D	E
f-CaO content in the mineral compositions/%	0.35	4.96	0.21	0.51	2.09
MgO content in the chemical compositions/%	7.68	3.46	6.54	5.98	5.15
Specific surface areas/kg m^{-3}	453	461	472	442	516

Under autoclaved condition, free CaO and the minerals containing MgO might react with the hydration of C_3S and C_2S. So the reaction of free CaO and the minerals containing MgO has a considerable influence on the hydration properties of steel slag under autoclaved condition.

In this paper, the hydration properties of steel slag under autoclaved condition were investigated, among which the reactions of free CaO and the minerals containing MgO are the key points concerned.

Experimental

Raw materials

Five steel slags were used in this paper. Table 1 shows the free CaO (*f*-CaO) contents, MgO contents, and specific surface areas of the five steel slags. It is obvious that there are significant differences among the *f*-CaO contents of the five steel slags, but the differences among the MgO contents are smaller. The specific surface areas of the five steel slags are close to each other. Portland cement with the strength grade of 42.5 complying with the Chinese National Standard GB 8076-2008 was used. The specific surface area of cement was 350 m^2 kg^{-1}. The MgO content of the cement used is 2.32 %.

Experimental procedure

Steel slag paste was prepared by mixing steel slag with water at the water-to-steel slag ratio of 0.3 (mass ratio). Cement paste was prepared by mixing cement with water at the water-to-cement ratio of 0.3 (mass ratio). Cement–steel slag paste was prepared by mixing cement, steel slag, and water at the water-to-binder (steel slag and steel slag) ratio of 0.3 (mass ratio).

(1) *Microscopic test* The steel slag paste and cement paste were cured at 20 °C for 3 h, and then, under the autoclaved condition (216 °C and 2 MPa) for 3 h. The morphologies of the autoclaved sample were observed by scanning electron microscopy (SEM). The chemical compositions of the hydration products of the autoclaved sample were measured by energy-dispersive X-ray (EDX). The TG–DTG curve of the autoclave sample was obtained by using a TA-Q5000 instrument with a heating rate of 10 °C min^{-1} in nitrogen atmosphere.

(2) *Expansion ratio* The cement–steel slag paste and cement paste were cured at 20 °C for 7 days. Then, the samples were cured under the autoclaved condition (216 °C and 2 MPa) for 3 h. The expansion ratio of the sample after autoclaved curing was measured.

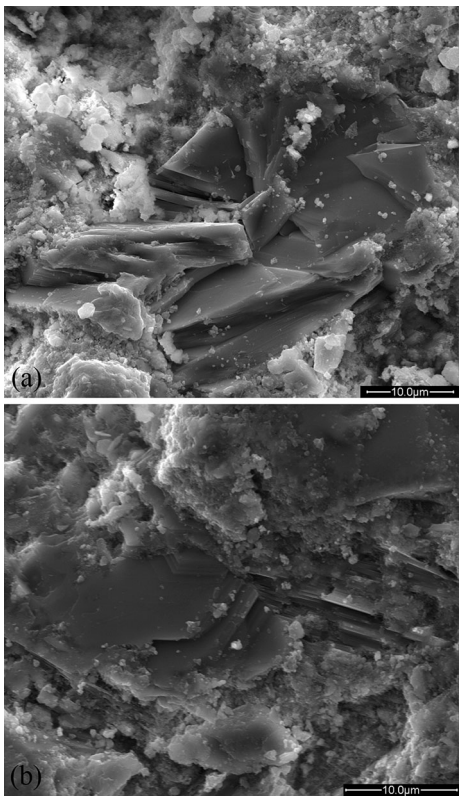

Fig. 1 Morphologies of the $Ca(OH)_2$ produced by cement

Results and discussion

Morphologies of the $Ca(OH)_2$

Figure 1 shows the morphologies of the products of cement after autoclaved curing. It is clear that there are a lot of

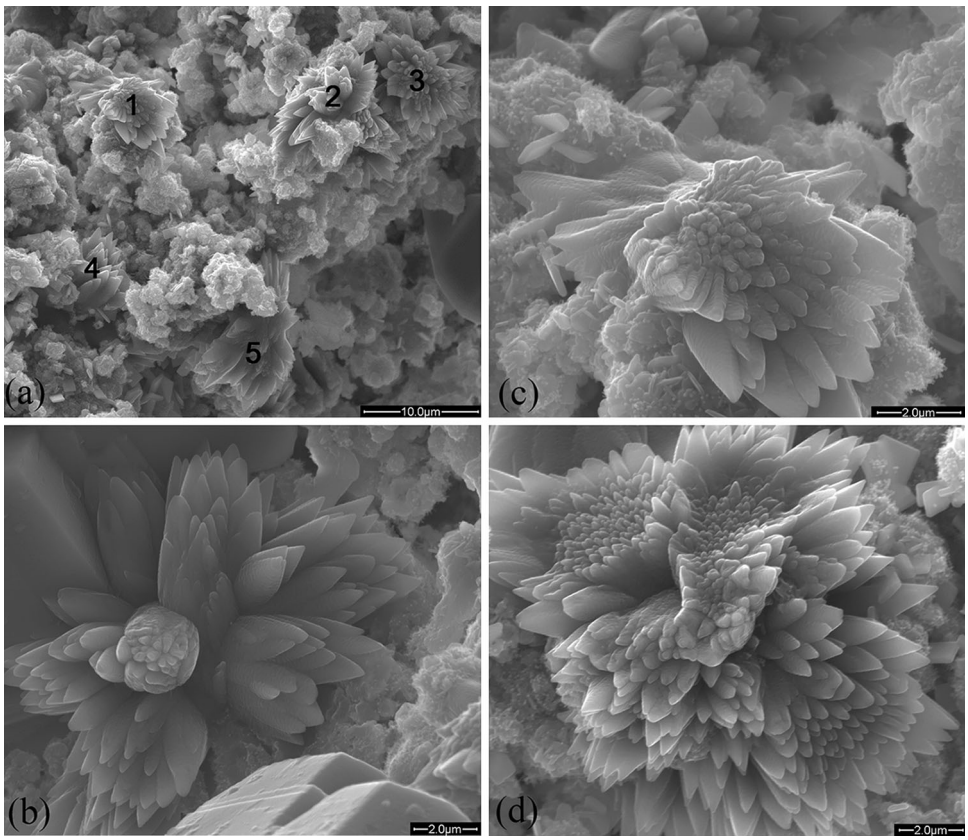

Fig. 2 Petal-shaped $Ca(OH)_2$ produced by steel slag

flakes or tabular crystals embedded in the C–S–H gel. It is easy to confirm that these crystals are $Ca(OH)_2$. The morphologies of the $Ca(OH)_2$ in Fig. 1 are very similar to those of the cement hydrating at normal temperature [21]. It is an indication that the morphologies of $Ca(OH)_2$ formed by the hydration of C_2S or C_3S at normal temperature and under autoclaved condition are very similar.

There are significant differences among the morphologies of the steel slag pastes after autoclaved curing. In the pastes of steel slag B and steel slag E, there are a lot of petal-shaped crystals embedded in the C–S–H gel (Fig. 2). Table 2 shows the chemical compositions of the crystals in Fig. 2a. Based on the data in Table 2, the crystals in Fig. 2a are $Ca(OH)_2$. The structures of the petal-shaped crystals can be seen more clearly in Fig. 2b–d. It is obvious that the specific surface area of the petal-shaped $Ca(OH)_2$ is much larger than that of the flake or tabular $Ca(OH)_2$. Therefore, it can be deduced that the formation of the petal-shaped $Ca(OH)_2$ tends to occupy considerable space and cause expansion. It should be pointed out that the petal-shaped $Ca(OH)_2$ is hardly observed in the pastes of steel slag A, steel slag C, and steel slag D. Note that the *f*-CaO contents of steel slag B and steel slag E are much higher than those of steel slag A, steel slag C, and steel slag D. It is an indication that the petal-shaped $Ca(OH)_2$ is the reaction product of *f*-CaO.

Table 2 Chemical compositions of the crystals in Fig. 2a/at.%

Samples	Ca	O	Mg	Al	Si	P	Fe
1	23.27	72.12	0.76	0.23	1.19	0.08	0.98
2	28.84	65.56	0.60	0.42	1.48	0.23	0.81
3	34.35	60.73	0.62	0.40	0.55	0.46	0.76
4	39.89	58.40	0.79	0.43	0.49	0	0
5	33.79	66.21	0	0	0	0	0

In the pastes of steel slag B and steel slag E, there are also a lot of big block-shaped crystals embedded in the C–S–H gel (Fig. 3). Table 3 shows the chemical compositions of the big block-shaped crystals in Fig. 3. It can be concluded from Table 3 that the big block-shaped crystals are $Ca(OH)_2$. The formation of these big block-shaped crystals might also cause expansion. Note that the big block-shaped $Ca(OH)_2$ is hardly observed in the pastes of steel slag A, steel slag C, and steel slag D, either. Thus, it can be concluded that the big block-shaped $Ca(OH)_2$ is also the reaction product of *f*-CaO.

$Ca(OH)_2$ is one of the main hydration products of steel slag. It is produced by the hydration of C_3S and C_2S as well as the reaction of *f*-CaO. Based on the above analysis, the morphologies of the $Ca(OH)_2$ produced by *f*-CaO are quite

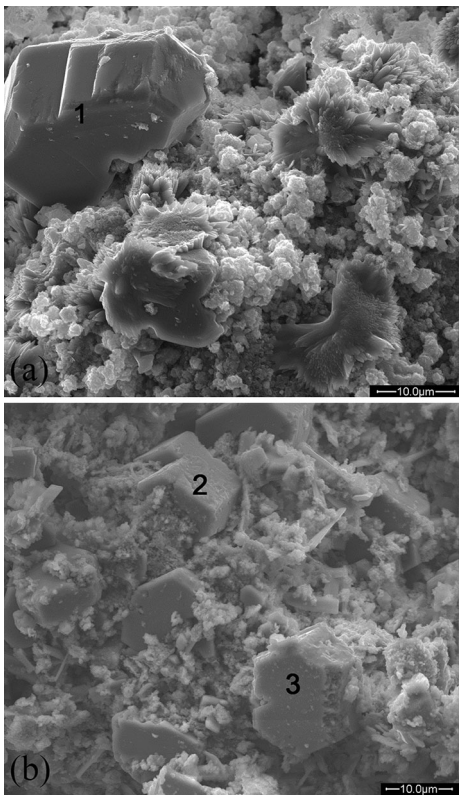

Fig. 3 Big block-shaped $Ca(OH)_2$ produced by steel slag

Table 3 Chemical compositions of the crystals in Fig. 3a, b/at.%

Samples	Ca	O	Mg	Al	Si
1	27.93	71.60	0.18	0.10	0.19
2	33.10	64.94	0.73	0.52	0.70
3	32.37	65.82	0.59	0.56	0.66

different from those of the $Ca(OH)_2$ produced by C_3S and C_2S. The $Ca(OH)_2$ produced by *f*-CaO tends to have a larger specific surface area or volume.

Morphologies of the $Mg(OH)_2$

In each of the steel slag paste after autoclaved curing, the crystals in Fig. 4 can be observed. Table 4 shows the chemical compositions of the crystals in Fig. 4a–d. It can be concluded from the data of Table 4 that the crystals in Fig. 4 are $Mg(OH)_2$. The shape of $Mg(OH)_2$ is irregular. The volume of $Mg(OH)_2$ is larger than that of MgO, so it is generally accepted that the formation of $Mg(OH)_2$ is a factor causing expansion [22, 23]. It should be pointed out that the $Mg(OH)_2$ crystals are much easier to be found in the steel slag paste than in the cement paste. This phenomenon is due to two reasons: (1) The MgO content of steel slag is higher than that of cement; (2) the C–S–H gel produced by the hydration of steel slag is much less than that produced by the hydration of cement.

Ca–Si ratio of C–S–H gel

The mole fractions of elements of C–S–H gel were calculated based on EDX analysis. For each sample, 40 micro-areas of C–S–H gel were tested. Figure 5 shows the mean Ca–Si ratios of C–S–H gel of the cement paste and steel slag pastes after autoclaved curing. According to Taylor [24], the mean Ca–Si ratio of the C–S–H gel of cement hydrating at normal temperature for 20 years is 1.84. Some literatures show that the mean Ca–Si ratio of the C–S–H gel of cement hydrating at normal temperature is between 1.5 and 2.0, and even higher [25–27]. It can be seen from Fig. 5 that the mean Ca–Si ratio of the C–S–H gel of the cement paste is close to 2.0, and those of the C–S–H gel of the steel slag pastes are between 1.7 and 1.9. Therefore, the difference of Ca–Si ratio of C–S–H gel between the cement cured at normal temperature and the cement cured under autoclaved condition is insignificant. In general, the Ca–Si ratio of C–S–H gel produced by steel slag is a little smaller than that produced by cement.

TG–DTG results

Figure 6a–e show the TG–DTG curves of steel slag A paste, steel slag B paste, steel slag C paste, steel slag D paste, and steel slag E paste after autoclaved curing, respectively. For each sample, there are three main endothermic peaks within 800 °C on the DTG curve: decomposition of $Mg(OH)_2$ (at about 300–400 °C); decomposition of $Ca(OH)_2$ (at about 400–500 °C); and decomposition of C–S–H gel (at about 550–650 °C). Based on the TG–DTG curves, the $Mg(OH)_2$ content and $Ca(OH)_2$ content in the hydration products can be calculated.

Figure 7 shows the relationship between MgO content in the chemical composition of steel slag and $Mg(OH)_2$ content in its hydration products. It is clear that the $Mg(OH)_2$ content in the hydration products is positively correlated with the MgO content in the chemical compositions. This is because the $Mg(OH)_2$ is completely from the reaction of the minerals containing MgO. It is an indication that the reaction of the minerals containing MgO is sufficient under autoclaved condition.

Figure 8 shows the relationship between *f*-CaO content in the mineral composition of steel slag and $Ca(OH)_2$ content in its hydration products. On the whole, the $Ca(OH)_2$ content in the hydration products is not positively correlated with the *f*-CaO content in the mineral composition. This is because the $Ca(OH)_2$ is from the reaction of *f*-CaO as well as the hydration of C_3S and C_2S. The $Ca(OH)_2$ content in the hydration products is close to 10 % even when the *f*-CaO content in the mineral composition is very low, indicating

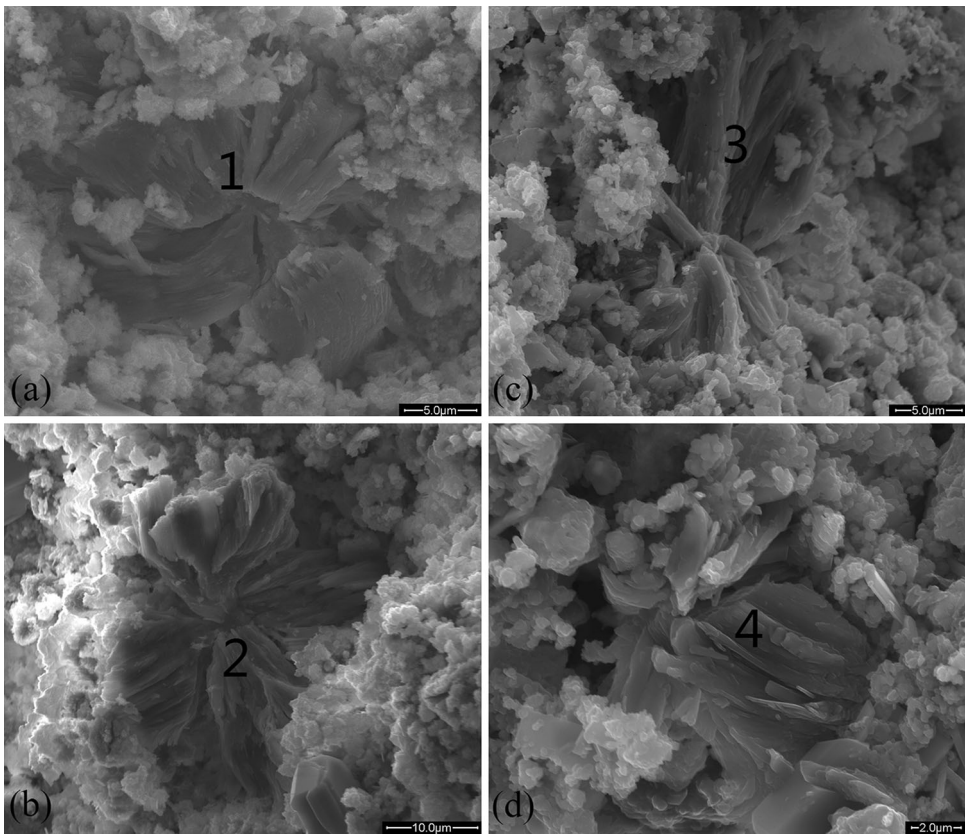

Fig. 4 $Mg(OH)_2$ produced by steel slag

Table 4 Chemical compositions of the crystals in Fig. 4a–d/at.%

Samples	Ca	O	Mg	Mn	Fe
1	0	57.46	35.06	1.26	6.22
2	0.86	54.11	38.25	2.12	4.66
3	0	56.91	38.12	0.75	4.22
4	1.70	51.44	35.79	2.45	8.62

that the hydration degree of C_3S and C_2S is very high under autoclaved condition. Figure 8 also shows that the $Ca(OH)_2$ content of steel slag B paste is much higher than those of the other steel slag pastes. Note that the *f*-CaO content of steel slag B is much higher than those of other steel slags (Table 1). Therefore, in the hydration of steel slag under autoclaved condition, the reaction of *f*-CaO makes considerable contribution to the $Ca(OH)_2$ content.

It can be concluded from the TG–DTG results that the hydration degrees of C_2S, C_3S, *f*-CaO, and minerals containing MgO of steel slag are all very high under autoclaved condition.

Expansion ratio results

In order to investigate the expansion law caused by the reaction of *f*-CaO and minerals containing MgO, fifteen

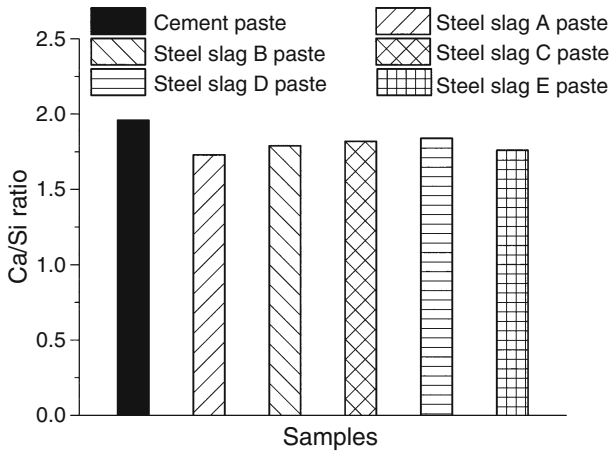

Fig. 5 Ca–Si ratios of the C–S–H gel produced by cement and steel slags

cement–steel slag pastes and one cement paste were prepared. Table 5 shows the compositions of the binders and the expansion ratios of hardened pastes after autoclaved curing. The reaction rate of *f*-CaO and minerals containing MgO is rather low at normal temperature, so it is acceptable that they hardly react after 7 days' curing at 20 °C. But after autoclaved curing, their reaction is sufficient. It can be seen in Table 5 that the expansion ratio of the cement paste is very

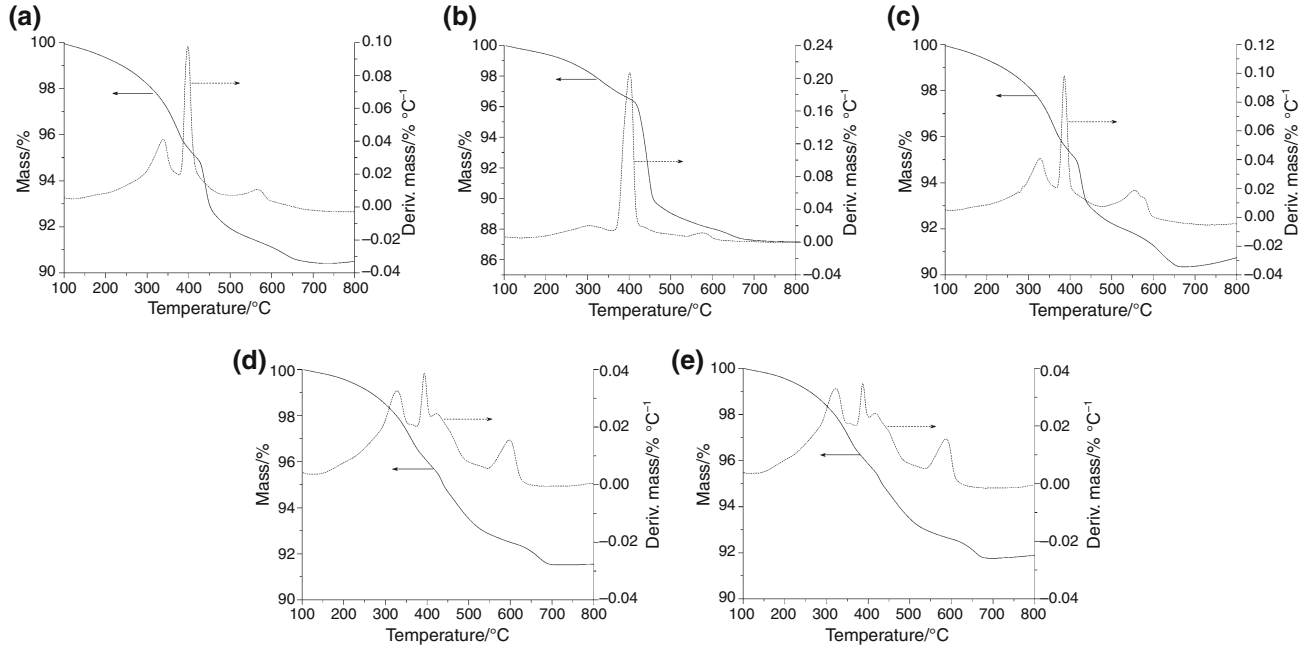

Fig. 6 TG–DTG curves of different pastes. **a** Steel slag A paste; **b** steel slag B paste; **c** steel slag C paste; **d** steel slag D paste; and **e** steel slag E paste

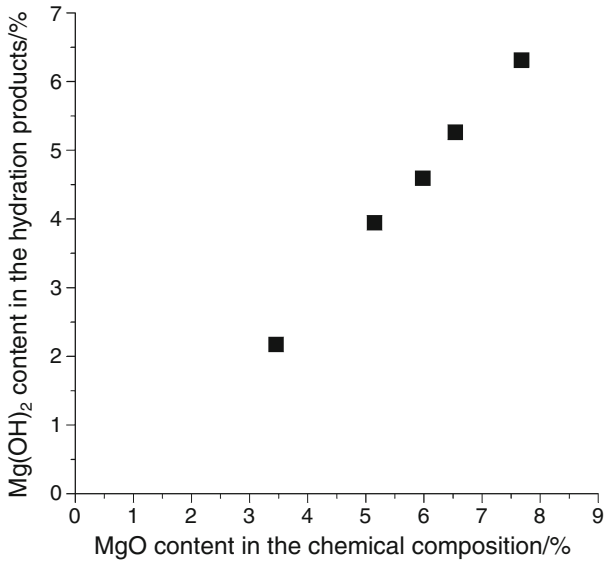

Fig. 7 Relationship between MgO content and $Mg(OH)_2$ content

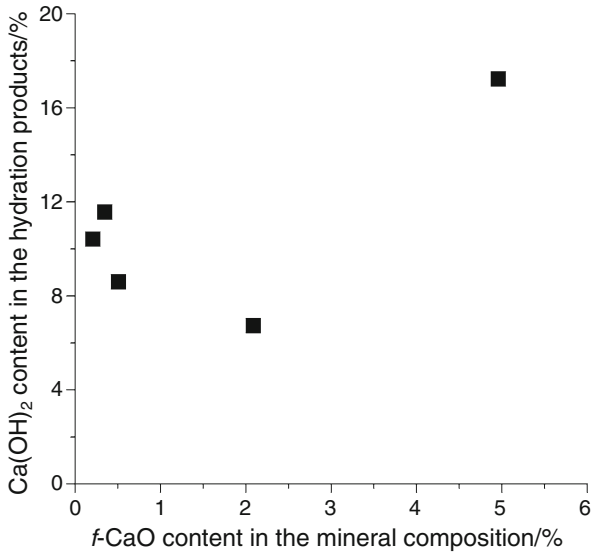

Fig. 8 Relationship between *f*-CaO content and $Ca(OH)_2$ content

small. But the expansion ratio increases significantly by replacing 15 % cement by steel slag B. When the replacements of cement by steel slag B are 30 and 50 %, the hardened pastes crack after autoclaved curing. Replacing cement by steel slag E also significantly influences the expansion ratio: The expansion ratio increases significantly in the cases of 15 and 30 % replacements; the hardened paste cracks after autoclaved curing in the case of 50 % replacement.

Table 5 also shows that the expansion ratio increases with the replacement of cement by steel slag A, or steel slag C, or steel slag D. However, when the replacement is 15 %, the expansion ratio increases slightly; when the replacement is 50 %, the hardened paste does not crack. It is obvious that under autoclaved condition, steel slag B and steel slag E tend to increase the expansion ratio more seriously than steel slag A, steel slag C, and steel slag D. What is more, steel slag B tends to increase expansion ratio more seriously than steel slag E. Therefore, it can be concluded from Tables 1 and 5 that under autoclaved condition, the reaction of *f*-CaO tends to increase expansion ratio more seriously

Table 5 Autoclave soundness of the binders

Composition of binder/%		Expansion ratio/%
Cement	Steel slag	
100	0	0.18
85	15 (steel slag A)	0.27
70	30 (steel slag A)	0.39
50	50 (steel slag A)	0.55
85	15 (steel slag B)	0.51
70	30 (steel slag B)	Cracked
50	50 (steel slag B)	Cracked
85	15 (steel slag C)	0.17
70	30 (steel slag C)	0.29
50	50 (steel slag C)	0.41
85	15 (steel slag D)	0.28
70	30 (steel slag D)	0.45
50	50 (steel slag D)	0.58
85	15 (steel slag E)	0.42
70	30 (steel slag E)	0.72
50	50 (steel slag E)	Cracked

than that of the minerals containing MgO. This might be because the $Ca(OH)_2$ produced by *f*-CaO has a larger specific surface area or volume than the $Mg(OH)_2$ produced by the minerals containing MgO.

Conclusions

(1) High curing temperature can excite the activity of steel slag. Under autoclaved condition, C_3S, C_2S, *f*-CaO, and the minerals containing MgO of steel slag can react sufficiently.

(2) Under autoclaved condition, the morphologies of $Ca(OH)_2$ produced by *f*-CaO are quite different from those of $Ca(OH)_2$ produced by C_3S and C_2S. The $Ca(OH)_2$ produced by *f*-CaO has a larger specific surface area or volume.

(3) Under autoclaved condition, the mean Ca–Si ratio of C–S–H gel produced by the hydration of steel slag is between 1.7 and 1.9, which is a little smaller than that produced by the hydration of cement.

(4) Under autoclaved condition, the reaction of *f*-CaO tends to cause larger expansion than that of the minerals containing MgO.

Acknowledgements Authors acknowledge the support from the State Key Laboratory of High Performance Civil Engineering Materials (2011CEM005) and Tsinghua University Initiative Scientific Research Program (20131089239).

References

1. Shi CJ. Steel slag-its production, processing, characteristics, and cementitious properties. J Mater Civil Eng. 2004;16:230–6.
2. Kourounis S, Tsivilis S, Tsakiridis PE, Papadimitriou GD, Tsibouki Z. Properties and hydration of blended cements with steelmaking slag. Cem Concr Res. 2007;37(6):815–22.
3. Tsakiridis PE, Papadimitriou GD, Tsivilis S, Koroneos C. Utilization of steel slag for Portland cement clinker production. J Hazard Mater. 2008;152:805–11.
4. Liu SH, Li LH. Influence of fineness on the cementitious properties of steel slag. J Therm Anal Calorim. 2014;117:629–34.
5. Hu SG, Wang HX, Zhang GZ, Ding QJ. Bonding and abrasion resistance of geopolymeric repair material made with steel slag. Cem Concr Compos. 2008;30(3):239–44.
6. Zhang TS, Yu QJ, Wei JX, Li JX, Zhang PP. Preparation of high performance blended cements and reclamation of iron concentrate from basic oxygen furnace steel slag. Resour Conserv Recycl. 2011;56(1):48–55.
7. Zhang TS, Liu FT, Liu SQ, Zhou ZH, Cheng X. Factors influencing the properties of a steel slag composite cement. Adv Cem Res. 2008;20:145–50.
8. Wang Q, Yan PY, Yang JW. Influence of steel slag on mechanical properties and durability of concrete. Constr Build Mater. 2013;47(10):1414–20.
9. Wang Q, Yan PY, Han S. The influence of steel slag on the hydration of cement during the hydration process of complex binder. Sci China Technol Sci. 2011;54(2):388–94.
10. Zhu X, Hou HB, Huang XQ, Zhou M, Wang WX. Enhance hydration properties of steel slag using grinding aids by mechanochemical effect. Constr Build Mater. 2012;29:476–81.
11. Li JX, Yu QJ, Wei JX, Zhang TS. Structural characteristics and hydration kinetics of modified steel slag. Cem Concr Res. 2011;41:324–9.
12. Yan PY, Mi GD, Wang Q. A comparison of early hydration properties of cement–steel slag binder and cement–limestone powder binder. J Therm Anal Calorim. 2014;115(1):193–200.
13. Qian GR, Sun DD, Tay JH, Lai ZY, Xu GL. Autoclave properties of kirschsteinite-based steel slag. Cem Concr Res. 2002;32:1377–82.
14. Yazıcı H, Deniz E, Baradan B. The effect of autoclave pressure, temperature and duration time on mechanical properties of reactive powder concrete. Constr Build Mater. 2013;42:53–63.
15. Hossain KMA. Volcanic ash and pumice as cement additives: pozzolanic, alkali–silica reaction and autoclave expansion characteristics. Cem Concr Res. 2005;35:1141–4.
16. Saphouvong K, Saito T, Otsuki N, Yumoto T. Corrosion of steel bars in autoclaved concrete pile containing γ-2CaO·SiO2 with an accelerated carbonation curing submerged in the real marine environment. J Soc Mater Sci. 2012;61(3):299–307.
17. Li H, Zhao FQ, Li Q, Fu LL, Liu SJ. Autoclave brick from semi-dry desulfuration ash. Adv Mater Res. 2011;846:217–8.
18. Connan H, Ray A, Thomas P, Guerbois JP. Effect of autocalving temperature on calcium silicate-based building products containing clay-brick waste. J Therm Anal Calorim. 2012;88:115–9.
19. Qian GR, Sun DD, Tay JH, Lai ZY. Hydrothermal reaction and autoclave stability of Mg bearing RO phase in steel slag. Br Ceram Trans. 2002;101(4):159–64.
20. Zhang TS, Yu QJ, Wei JX, Li JX. Investigation on mechanical properties, durability and micro-structural development of steel slag blended cements. J Therm Anal Calorim. 2012;110:633–9.
21. Mindness S, Young JF. Concrete. New Jersey: Englewood Cliffs; 1981. p. 93–4.

22. Gao PW, Wu SX, Lu XL, Deng M, Lin PH, Wu ZR, Tang MS. Soundness evaluation of concrete with MgO. Constr Build Mater. 2007;21(1):132–8.
23. Ali MM, Mullick AK. Volume stabilization of high MgO cement: effect of curing conditions and fly ash addition. Cem Concr Res. 1998;28:1585–94.
24. Taylor R, Richardson IG, Brydson RMD. Composition and microstructure of 20-year-old ordinary cement-ground granulated blast-furnace slag blends containing 0 to 100% slag. Cem Concr Res. 2010;40:971–83.
25. Richardson IG. The nature of C–S–H in hardened cements. Cem Concr Res. 1999;29:1131–47.
26. Escalante-Garcia JI, Mendoza G, Sharp JH. Indirect determination of the Ca–Si ratio of the C–S–H gel in Portand cements. Cem Concr Res. 1999;29:1999–2003.
27. Gutteridge WA, Dalziel JA. Effect of a secondary component on the hydration of Portland cement, Part I: a fine non-hydraulic filler. Cem Concr Res. 1990;20:778–82.